Article ID: 1006-8775(2000) 02-0162-10

SOUTH CHINA REGIONAL SHORT RANGE CLIMATE PREDICTION MODEL AND ITS PERFORMANCE

YAN Jing-hua (闫敬华)

(*Guangzhou Institute of Tropical and Oceanic Meteorology, Guangzhou,* 510080 *China*)

ABSTRACT: In this paper, a newly established "South China Regional Short Range Climate Prediction Model System" is introduced and its performance is analyzed in real case simulation. It shows that the system has a good performance and suitable for short range climate modeling. The model simulates well the monthly mean, pentad mean and daily field, pentad mean and daily field and can depict more details than coarse resolution analyses. Weather systems and information can pass into and out of the model domain through lateral boundaries without notable damping. Almost all of the weather and climate changes can be reflected in the simulation, in which both the changing tendencies, amplitudes, speeds, and phases are consistent with the real cases. The simulated precipitation is much close to the observed one, both in the extent, position and in the intensity of rainfall. In addition, some smaller precipitation centers could also be reflected in the simulation.

Key words: regional short-range climate model; real case simulation; performance

CLC number: P435 **Document code:** A

1 INTRODUCTION

Short-term numerical predictions of climate are those conducted dynamically for short-term climate, mainly on the scales of the month and season, using numerical prediction models. Surpassing limits of definite predictability as they apparently are, predictions on these scales do carry real significance if they have been properly pre-processed, such as filtering of initial values, ensemble forecasting, and post-processing of outputs, etc, during the prediction procedure, as shown in much research work. Over the past few years, the numerical method has been used across the world as one of the important means in research and operation for the prediction of short-term climate. Since mid-1980's, a large amount of monthly scale prediction experiments have been satisfactorily conducted in large world centers such as ECMWF (Tibalki, Palmer and Brakkovic, 1990), NMC of the United States, Climate Center of Canada and JMA of Japan (Zhang, Ji and Li, 1996). Wider use is found with the regional climate model to cope with the issue of predicting and studying short-term climate, exploying the advantages and necessity they carry. Good modeling and predicting results have been achieved with numerical prediction systems completed in U.S.A. and Germany for regional short-term climate. The second generation of the system has been operational at NCAR (Giorgi, Marinucci and Canio, 1993b). A large amount of numerical modeling and research has also been done in China in this aspect (Liu, Ding, Zhao, 1996; Zhao, Luo and Leung, 1997). All of these efforts are suggesting that regional climate models are

Received date: 1999-05-25; **revised date:** 2000-07-17

Foundation item: A core scientific research project in the national 9th five-year economic development plan (96-908-05-07)

Biography: YAN Jing-hua (1963 –), male, native from Longchuan County Yunnan Province, professor at Guangzhou Institute of Tropical and Oceanic Meteorology, Master degree holder, undertaking the study of numerical prediction and low-latitude weather and climate.

good at simulating and predicting short-term climate. The regional model presented in this work is a numerical one that has been improved over previous research findings and modified with operational environment and realistic conditions of the southern China, with inclusion of internationally advanced numerical models. The system is now completed and its performance tested by simulating real cases.

2 BRIEF ACCOUNT OF MODEL

The model in use is the so-called "short-term climate prediction model for the region of South China" that has been developed lately at the institute. It has been developed from a mesoscale model introduced from the German Meteorological Services (Majewski, 1991). The model is characterized by the following points:

2.1 *Use of mixed co-ordinates in vertical ordinate*

In the coordinate, we have

$$P = A(\sigma) + P_s B(\sigma)$$

$$A(\sigma) = P_0 \sigma, \quad B(\sigma) = 0 \qquad \text{(when } 0 \leqslant \sigma \leqslant \sigma_T \text{)}$$

$$A(\sigma) = \frac{P_0 P_T}{P_0 - P_T}(1-\sigma), \quad B(\sigma) = \frac{P_0 \sigma - P_T}{P_0 - P_T} \qquad \text{(when } \sigma_T \leqslant \sigma \leqslant 1\text{)}$$

where P_0 = 1000 hPa, P_T takes 220 hPa and $\sigma_T = P_T / P_0 = 0.220$.

The $\dot{\sigma}$ coordinate absorbs the advantages of the *P* coordinate and σ coordinate while at the same time avoids their shortfalls. The elements *u*, *v*, *t*, *q* are defined at the center of a layer and *h*, σ on the surface dividing layers. At present, the model is divided into 20 layers that are not at equal intervals and covered with not any tops; and there are 5 ~ 6 more layers within the boundary layer with the upper and lower lateral conditions of $\dot{\sigma}$=0 (σ=0 or σ=1).

2.2 *Use of "rotation latitude-longitude mesh" system in horizontal ordinate*

Rotating at a given "Eular angle", the geographic North Pole is displaced to a new position so that the equator after rotation goes through the central region of the model. The factor of scale varies little within the model domain, making it easier to take larger time steps.

The rotation coordinates (φ', λ') is related to the geographic coordinates (φ, λ) by the expressions of

$$\lambda = \lambda_N - \arctan\left(\frac{\cos\varphi' \sin\lambda'}{\sin\varphi' \cos\varphi_N - \cos\varphi' \sin\varphi_N \cos\lambda'}\right)$$

$$\varphi = \arcsin\left(\cos\varphi_N \cos\lambda' \cos\varphi' + \sin\varphi_N \cos\lambda'\right)$$

$$\lambda' = \arctan\left(\frac{-\cos\varphi \sin(\lambda - \lambda_N)}{-\sin\varphi_N \cos\varphi \cos(\lambda - \lambda_N) - \cos\varphi_N \sin\varphi}\right)$$

$$\lambda' = \arcsin\left(\cos\varphi_N \cos\varphi \cos(\lambda - \lambda_N) + \sin\varphi_N \cos\varphi\right)$$

where λ_N, φ_N is the longitude and latitude of the North Pole in the rotation coordinates.

Corresponding wind fields are related by

$$U' = U\cos\delta - V\sin\delta$$

$$V' = U\sin\delta + V\cos\delta$$

$$U = U'\cos\delta + V'\sin\delta$$

$$V = -U'\sin\delta + V'\cos\delta$$

$$\delta = a\tan\left(\frac{\cos\varphi_N \sin(\lambda_N - \lambda)}{\cos\varphi \sin\varphi_N - \sin\varphi\cos\varphi_N \cos(\lambda_N - \lambda)}\right)$$

with the parameter for Coriolis force $f = 2\Omega\left(\sin\varphi'\sin\varphi_N + \cos\varphi'\cos\varphi_N\cos(\lambda' - \lambda_N)\right)$.

2.3 *Use of T, q instead of h, q_{DW} in thermodynamic and moisture conservation equations*

The treatment is

$$\frac{\partial h}{\partial t} = -\frac{1}{a\cos\varphi}\left(u\frac{\partial h}{\partial \lambda} + v\cos\varphi\frac{\partial h}{\partial \varphi}\right) - \dot{\eta}\frac{\partial h}{\partial \eta}$$

$$+ \alpha w + F_H^h - g\left(\frac{\partial P}{\partial \eta}\right)^{-1}\frac{\partial \eta_h}{\partial \eta} + \left(\frac{\partial h}{\partial t}\right)_{sub} - m_R(h - h_R)$$

$$\frac{\partial q_{DW}}{\partial t} = -\frac{1}{a\cos\varphi}\left(u\frac{\partial q_{DW}}{\partial \lambda} + v\cos\varphi\frac{\partial q_{DW}}{\partial \varphi}\right) - \dot{\eta}\frac{\partial D_{DW}}{\partial \eta}$$

$$+ F_H^{Q_{DW}} - g\left(\frac{\partial P}{\partial \eta}\right)^{-1}\frac{\partial \eta_{Q_{DW}}}{\partial \eta} + \left(\frac{\partial Q_{DW}}{\partial t}\right)_{sub} - m_R(Q_{DW} - Q_{DWR})$$

$$h = c_p T + L_V q_D$$

$$q_{DW} = q_D + q_W$$

where h is the total specific heat, q_D, q_W are specific humidity and specific cloud water content, and q_{DW} is the total water content. By the diagnostic equation, T, q_D and q_W are sought from h and q_{DW} so that there is one less prediction equation.

The whole frame of equations consist of 5 prediction equations and 11 diagnostic equations, which have 16 corresponding variables of direct prediction and diagnosis to form an enclosed set of equations.

2.4 *Use of Davies Scheme in lateral nesting (Davies, 1976)*

The scheme follows: $\frac{\partial y}{\partial t} = RHS - m_R\left(y - y_R\right)$

where y is the element predicted, RHS is the term in the right hand side of the prediction equation (without considering relaxation of lateral conditions), m_R is the relaxation coefficient for boundary nesting and y_R is the value of the lateral boundary to be determined by the driving model.

By implicit treatment of the relaxation term, unstable boundary nesting can be avoided, i.e.,

$$\frac{y^{t+\Delta t} - y^{t-\Delta t}}{2\Delta t} = RHS - m_R\left(y^{t+\Delta t} - y_R^{t+\Delta t}\right)$$

$$y^{t+\Delta t} = (1-\alpha)\tilde{y}^{t+\Delta t} + \alpha y_R^{t+\Delta t}$$

where $\tilde{y}^{t+\Delta t} = y^{t-\Delta t} + 2\Delta t RHS$ is the prediction that does not have relaxed boundary conditions.

On the other hand, $\alpha = \frac{2m_R\Delta t}{1+2m_R\Delta t}, m_R = \frac{\alpha}{1-\alpha}\frac{1}{2\Delta t}$, which shows that the relaxation effect of the boundary is contributed by the regional model prediction ($\tilde{y}^{t+\Delta t}$) and driving model prediction ($y^{t+\Delta t}$). Specifically, the value of the weighting coefficient α is determined by the following expression, which decreases from unity at the boundary to zero in the inner section of the regional model.

$$\begin{cases} \alpha_i = 1 - \tanh\left(0.5\frac{d_i}{\Delta}\right) & i = 1,2,\wedge,8 \\ \alpha_0 = 1 \end{cases}$$

d_i is the distance between i and the boundary, and Δ is the grid intervals. The boundary buffer zone takes 8 circles. Such definition has one shortfall, i.e., m_R is related with Δt. Therefore, m_R is defined not to be relevant with Δt.

$$\left(m_R\right)_i = \frac{1}{2\Delta t}\frac{\alpha_i}{1-\alpha_i}\frac{\Delta t}{300}\frac{0.5}{\max(\Delta l, \Delta j)}$$

Due to limited disk space and other operational conditions, the driving model (T106) updates the boundary value y_R every 6 to 12 hours and for the time steps between any two updates y_R is determined by linear interpolation.

The regional climate model is long valid in integration prediction, which is controlled decisively by the quality of boundary nesting. It is therefore necessary to minimize the error of y_R. To alleviate any errors intrigued by the decrease of interpolated values or any discrepancies they cause with the regional model, the following technical treatment has been conducted by procedures of

(1) selecting a larger model domain to which the driving model supplies $y_{R'}$;

(2) initializing larger-domain model (by normal mode) to filter out noises and set up a more coherent relationship among the elements, and
(3) removing several circles of boundary in the obtained larger-domain model that has been initialized to derive the boundary value y_R needed in the regional model.

2.5 *Treatment of temperature at ground surface*

The regional model contains complete land-surface processes based on which good forecasts can be made of temperature at ground surface, though with the absence of air-sea couplings. As a result, the temperature at the ocean surface adopts the time-dependent values (or time-dependent observations) provided by the driving model while that at the ground surface is taken care of by regional model itself.

2.6 *Schemes of physical processes included in the model*

The model takes a 4^{th}-order linear horizontal diffusion scheme, applies orographic correction with regard to the diffusion of total amount of heat, and takes into account of grid-scale precipitation having parameterized microphysics. In addition, Tiedtke's mass flux scheme (Tiedtke, 1989) for cumulus parameterization is used. For the vertical diffusion, a scheme by Louis (1979) is used for the near-surface layer and another dealing with the second-order matrix of the planetary boundary layer by Mellor and Yamada (1974) for the layers above it. Also included in the model is a complete long- and short-wave flux scheme for radiation by Ritter and Geleyn (1992), which contains a complete package of cloud-radiation feedback, and a 3-layer soil model by Jacobsen and Heise (1982), which takes complex land-surface effect into account. The model is horizontally resolved at 0.5°, composed of 81×73 grids in a domain of 95°E ~ 135°E and 8°N ~ 44°N and distributed over 20 layers. It meets operational requirements on the duration of validity because it needs about 10 hours of CPU to integrate for a month on our SGI-R10000 workstation.

3 ANALYSIS OF SIMULATION PERFORMANCE OF REAL CASES

In the real-case simulation, the initial field starts at 1200 UTC on 1 February 1998 and the integration predicts forward for a month (28 days). The driving model (T106) provides 12-h updates of boundary values. It is shown in the simulation that the regional model works well to give consistent results with the observation.

3.1 *Monthly mean and day-to-day simulation*

As seen in the monthly mean field (Fig.1), simulations are quite agreeable with observations in the geopotential height field and wind field on the upper (100 hPa), middle (500 hPa), and lower (850 hPa) levels. The simulated field is able to reproduce details too fine for low-resolution fields of observation to depict, for example, an enclosed cyclonic circulation is simulated at 850 hPa over the Sichuan Basin, which is consistent with the local climatic features. In contrast, only a transverse-trough-pattern shear is analyzed in the observed data. On the other hand, larger differences occur between the simulation and observation for the South China Sea and Indochina Peninsula. It is caused by lack of observations throughout the place and the difference is therefore not sufficient to account for the less desirable performance of the model.

For the pentad-to-pentad predictions, the simulation is shown to go conformably with the observation as in the case of monthly mean, suggesting that climatic information can be transported from the driving model to the regional model through the nested boundary without any significant

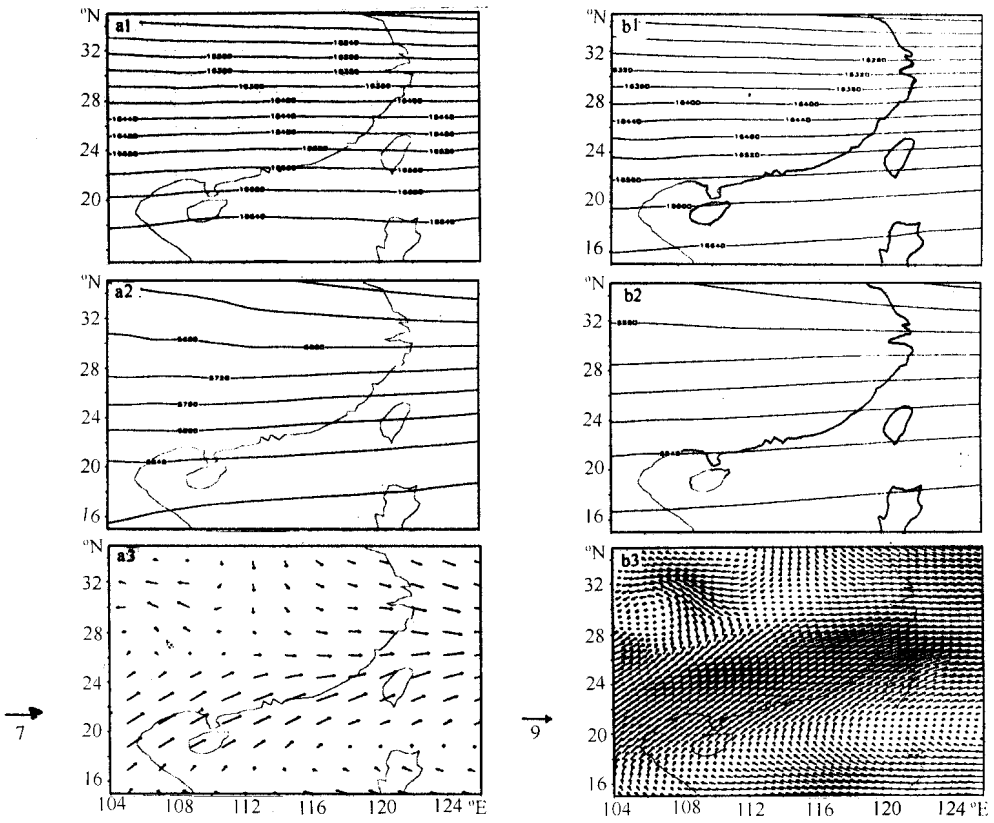

Fig.1 Monthly mean fields for February 1998. a: T106 analysis; b: model simulation. The numerals 1, 2, and 3 represent 100 hPa and 500 hPa heights, and 850 hPa winds respectively

noise. The situation of Pentad Three is given to illustrate (Fig.2). It shows that the prediction is almost identical with the observation in both the pattern and magnitude in addition to description of more details than the "observation" does, such as the cyclonic circulation over the Sichuan Basin and the high ridge over the South China Sea.

For a regional climate model, one of the essential prerequisites is that the weather and climate information contained in its driving model be transmitted to the regional model without any resistance while synoptic regimes in the regional model be moved without obvious reflection. As indicated in day-to-day predictions, every single synoptic process moves in and out of the boundary area of the regional model with no apparent resistance. In the forecasting for the whole month, prediction fields are basically the same as the observation for every lengths of validity. Take the forecast field on Day 28 for example (Fig.3). Except in some parts (such as the wind field over the Philippine Sea) of the waters, the prediction fixes so well with the observation that the winds are simulated with fitting precision in the wind speed, saying nothing of much finer description of air flows near Taiwan and anti-cyclonic circulation around the Island of Hainan. It shows how effective and suitable the scheme of lateral boundary nesting of the current system is.

3.2 S*imulation of evolution of weather systems*

Fig.4 gives the latitude-time profiles at 500 hPa along 114.5°E. It is clear from the figure that

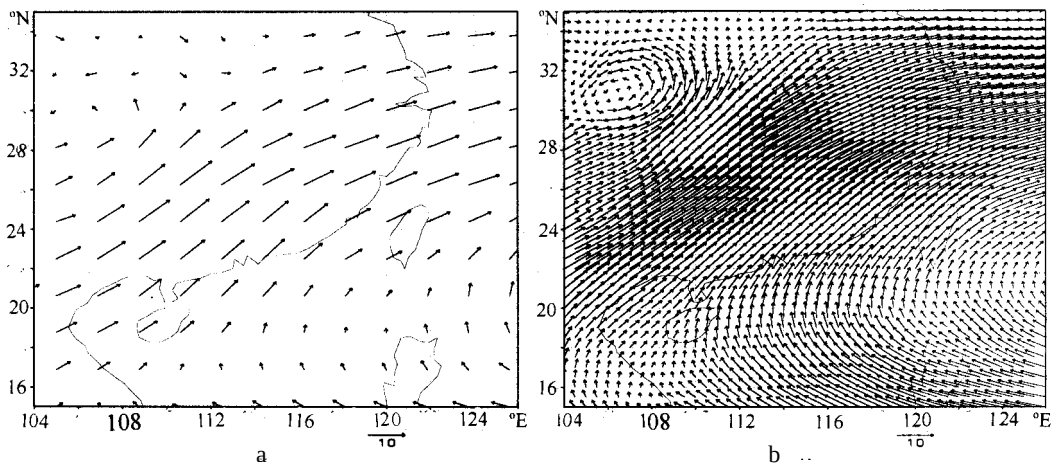

Fig. 2 Mean wind fields on 850 hPa for Pentad Three of February 1998. a: T106 analysis; b: model simulation.

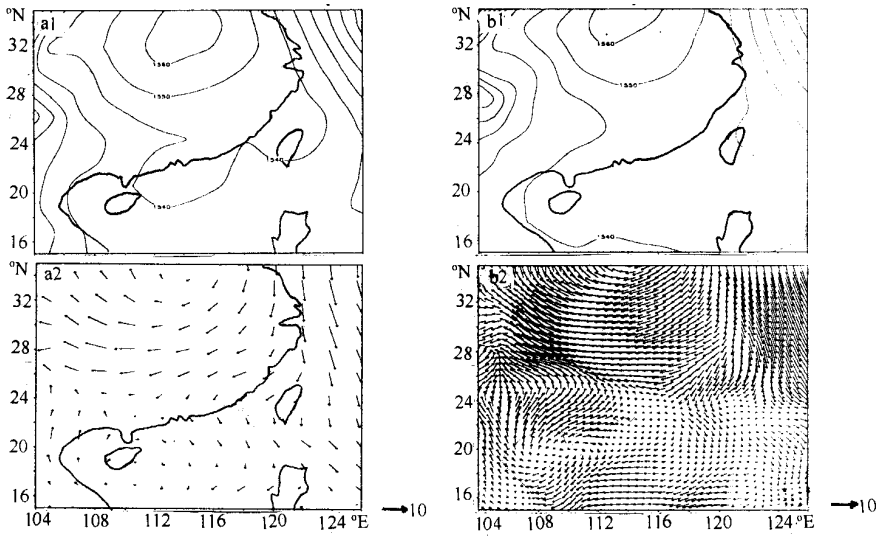

Fig.3 Fields on 850 hPa at 1200 UTC February 28, 1998. a: T106 analysis; b: model simulation. 1: heights; 2: winds.

the temporal evolution simulated is highly consistent with the observation. For example, the simulation is successful in presenting the deepening and southward movement of troughs on February 6, 18, and 26, the activity of ridges around February 13 and 16, and the activity of shallow troughs on February 14, etc.

Differences of varying degrees do exist though the model simulates a number of fine details of the evolution. For instance, the evolution differs obviously from the observation on February 1 ~ 2. It may be directly related with the lack of assimilated initial values in the regional model, which shows the importance of the initialization procedure. It also suggests that the initialization has governed the prediction for the first 1 ~ 2 days and the boundary nesting controlled it in periods afterwards in short-term regional climate model. Another major difference is around February 19, when it is in a time without boundary driving data (1200 UTC of February 19 and 0000 UTC of February 20). It is suggested that information at the boundary is swiftly transferred to the inner

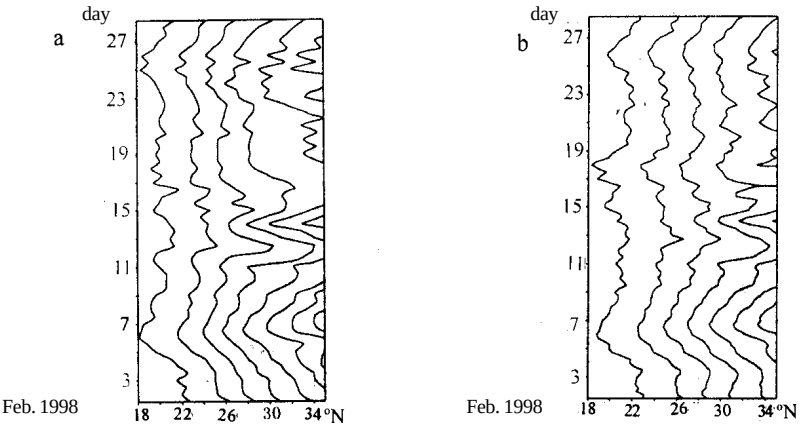

Fig.4 Latitude-time profile along 114.5°E at 500 hPa geopotential height in February 1998. a: T106 analysis; b: model simulation.

region of the model and the lateral boundary conditions play a key role in the regional short-term climate prediction.

The forecasting of precipitation is the most important and difficult part in the prediction of short-term climate. As shown in the study (figure omitted), the model gives good results concerning the pentad-to-pentad and decade-to-decade precipitation in addition to forecasts being generally consistent with the reality, specifically, the coverage of rain-falling area, central falling area, border area of the rain and amount of the rain. Fig.5 gives the total amount of precipitation on a monthly basis. The simulations indicate that the rainfall centers in northern Fujian province through eastern Guangxi Autonomous Region with much less falling north of 30°N and the South China Sea, being largely the same with the observation. Even a small center of precipitation in western Guangxi is predicted. In general, the rainfall is forecast to be generally a little heavier except for the Island of Taiwan where it rains by a less amount.

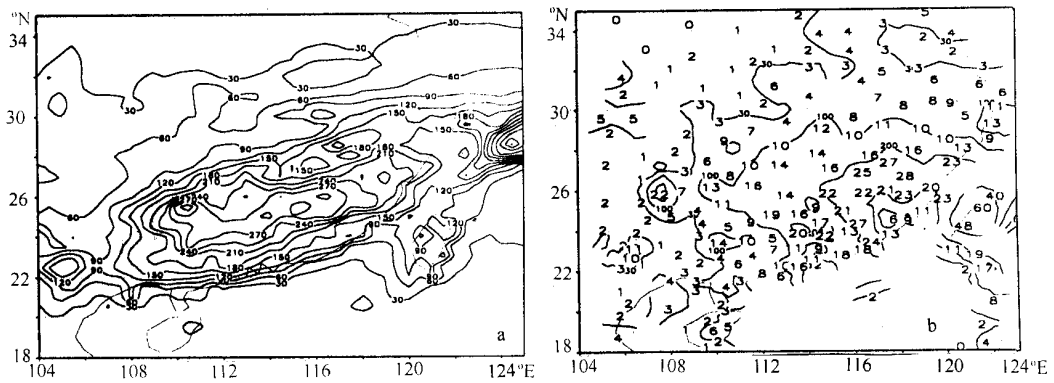

Fig.5 Accumulated precipitation for February 1998. a: model simulation (mm); b: observation (cm)

3.3 S*imulation of evolution of ground-surface elements*

Fig.6a is the 1-day running mean curve of pressure-time evolution at ground surface for Guangzhou, in which the variations of diurnal and fine scale cycles have been filtered out. The figure shows that the simulated pressure changes are basically the same with the observation, e.g.,

two large pressure rises on February 5 and 22, a gradual pressure drop on February 6 ~ 17, and another pressure rise on February 28. The model does a good job in simulation though with a systematic error of about 2 hPa. Fig.6b is the corresponding1-day running mean curve of 6-hourly amount of precipitation for the observation station in Guangzhou. All of the raining processes are forecast with magnitudes comparable to the reality. Examples are seen in the cases of February 5 and time around it, February 13 ~ 18, and February 22 ~ 28, and the model is also accurate in predicting the rain peaks, such as those on February 5, 18, and 26. Good forecasts are made for periods without any precipitation, like February 1 ~ 2 and February 7 ~ 12. A major false prediction is recorded for February 20 ~ 21, which may be caused by lack of boundary data nesting on February 19.

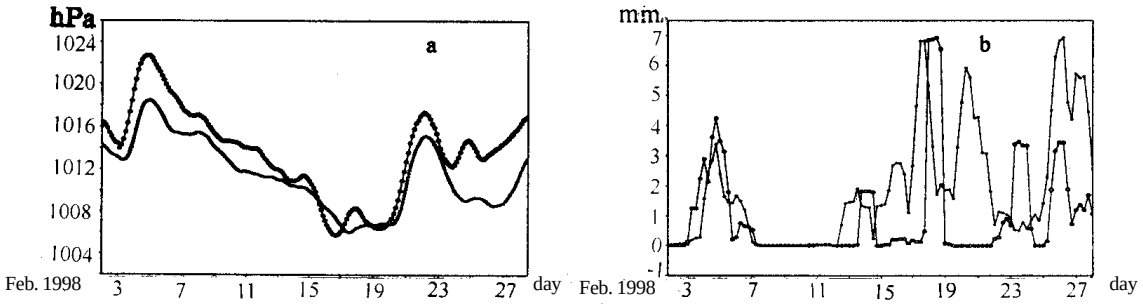

Fig.6 Time evolution of 1-day running mean curve of ground-surface elements at Guangzhou observation station in February 1998. a: surface pressure; b: 6-hourly precipitation (mm). Hollow dots: observed; solid dots: simulated

4 CONCLUDING REMARKS

a. The model system performs well in the monthly scale modeling and fits short-term climatic prediction for the south of China.

b. The monthly mean and pentad-to-pentad mean fields (basic flow) simulated are generally consistent with the observation with descriptions of more details.

c. The lateral boundary values and boundary nesting are playing a much larger role than the initial values for the regional climatic model prediction. The scheme used in this system to nest the boundary makes it easier for the weather information to pass through the model domain without any obvious resistance. The model is efficient and suitable for simulating the evolution of transient waves in major weather events.

d. The model is useful in simulating the temporal evolution of precipitation on a pentad and monthly basis with the area, location and intensity of the rain consistent with the observation, reflecting all rains and minor centers of precipitation.

e. The model exhibits good performance in simulating the evolution of ground-surface elements at single stations, reflecting almost all processes of weather and climate changes and presenting close-to-observation trends, amplitudes, velocities, and phases in these variations.

Acknowledgements: It is much appreciated that Mr. CAO Chao-xiong, who works at the Guangzhou Institute of Tropical and Oceanic Meteorology, has translated our paper into English.

REFERENCES:

DAVIES H C, 1976. A lateral boundary formulation for multi-level prediction models [J]. *Quart. J. R. Me-*

teor.Soc., **102**: 405-418.

GIORGI F, MARINUCCI M R, CANIO G De, et al., 1993b. Development of a second generation regional climate model (RegCM2) II: convective processes and assimilation of lateral boundary conditions [J]. *Mon. Wea. Rev*., **121**: 2814-2832.

JACOBSEN I, HEISE E, 1982. A new economic method for the computation of the surface temperature in numerical models [J]. *Beitr. Phys. Atmos.*, **55**: 128-141.

LIU Yong-qiong, DING Yi-hui, ZHAO Zong-ci, 1996. Simulation of regional climate concerning excessive heavy rains in the basin of the Changjiang and Huaihe River in 1991 [A]. *In*: Modeling research of short-term climate prediction in China [C]. Beijing: Meteorological Press, 106-120.

LOUIS J F, 1979. A parametric model of vertical eddy fluxes in the atmosphere [J]. *Boundary-Layer Meteor.*, **17**: 187-202.

MAJEWSKI D, 1987. The Europa-model of the deutscher wetterdiaenst [A]. ECMWF Seminar on numerical methods in atmospheric models [C], **2**: 147-191.

MELLOR G L, YAMADA T, 1974. A hierarchy of turbulence closure models for planetary boundary layers [J]. *J. Atmos. Sci.*, **31**: 1791-1806.

RITTER B, GELEYN J F, 1992. A comprehensive radiation scheme for numerical weather prediction models with potential applications in climate simulations [J]. *Mon. Wea. Rev*., **120**: 303-325.

TIBALKI S, PALMER T N, BRANKOVIC C, et al., 1990. Extended-range predictions with ECMWF models: influence of horizontal resolution on systematic error and forecast skill [J]. *Quart. J. Roy. Meteor. Soc.*, **116**: 835-866.

TIEDTKE M, 1989. A comprehensive mass flux scheme for cumulus parameterization in large-scale models [J]. *Mon. Wea. Rev*., **177**: 1779-1800.

YAN Jing-hua, 1999. A time filtering scheme for the short range climate prediction model products and its real case analysis [J]. *J. Trop. Meteor*.(Chinese Ed.), **15** (3): 213-220.

ZHANG Dao-min, JI Li-ren, LI Jin-long, 1996. Experimental study of monthly numerical predictions [A]. *In*: The simulation and prediction of catastrophic climates [C] Beijing: Meteorological Press, 1-11.

ZHAO Zong-ci, LUO Yong, LEUNG R, et al., 1997. Simulation of summer monsoon over east Asia: intercomparisons of three regional climate models [J]. *Quar. J. Appl. Meteor.*, **8** (suppl.): 116-123.